Experimental evidence of reaction-driven miscible viscous fingering

L. A. Riolfo,[1] Y. Nagatsu,[2] S. Iwata,[2] R. Maes,[1] P. M. J. Trevelyan,[1] and A. De Wit[1]

[1]*Nonlinear Physical Chemistry Unit, Faculté des Sciences, Université Libre de Bruxelles (ULB), CP231, 1050 Brussels, Belgium*

[2]*Department of Materials Science and Engineering, Graduate School of Engineering, Nagoya Institute of Technology,*

Gokiso-cho, Showa-ku, Nagoya, Aichi 466-8555, Japan

An experimental demonstration of reaction-driven viscous fingering developing when a more viscous solution of a reactant A displaces a less viscous miscible solution of another reactant B is presented. In the absence of reaction, such a displacement of one fluid by another less mobile one is classically stable. However, a simple $A + B \to C$ reaction can destabilize this interface if the product C is either more or less viscous than both reactant solutions. Using the pH dependence of the viscosity of some polymer solutions, we provide experimental evidence of both scenarios. We demonstrate quantitatively that reactive viscous fingering results from the buildup in time of nonmonotonic viscosity profiles with patterns behind or ahead of the reaction zone, depending on whether the product is more or less viscous than the reactants. The experimental findings are backed up by numerical simulations.

Viscous fingering (VF), also often referred to as the Saffman-Taylor instability, appears when a fluid with a given viscosity displaces another more viscous and hence less mobile one in porous media. This hydrodynamic instability has been largely studied both theoretically and experimentally [1–4] because of the beauty and generic character of the ramified patterns produced but also because of its practical consequences. VF is indeed observed in applications as diverse as hydrology [5,6], petroleum recovery [1], liquid crystal [7] or polymer processing [3,8–11], and separation techniques [6], to name a few. In general, the focus is classically on the unstable displacement of a fluid by a less viscous one. We show here that chemical reactions can destabilize the reverse case.

Some experimental [12–15] and theoretical [16–22] studies have shown that a chemical reaction, by modifying the viscosity of the solutions at hand, can influence miscible VF. Theoretical work [21,22] has, however, suggested that reactions could even destabilize the classically stable reverse situation of a more viscous fluid displacing a less viscous one. To do so, it has been predicted that the product of the reaction must have a viscosity either larger or smaller than the viscosity of the reactants.

In this work we present experimental evidence of such reaction-driven VF destabilization of a more viscous liquid displacing a less viscous one. We show quantitatively that the classically stable interface between a viscous reactant A pushing a less viscous aqueous solution of another reactant B can be destabilized by the buildup through a reaction of nonmonotonic viscosity profiles in time. The experimental study is carried out using aqueous solutions of polymers, chosen mainly because of their viscosity dependence on pH. If a solution of such a polymer A displaces less viscous dyed water, no instability is obtained and the interface remains planar. However, upon addition of a pH changing reactant B in the displaced water, an $A + B \to C$ neutralization reaction generates a product C either more viscous than the polymer A or less viscous than the solution of B triggering reaction-induced fingering. We provide experimental realization of both scenarios, and explain the origin of the destabilization by quantitative measurements of viscosities and numerical simu-

lations. We also highlight the difference between VF patterns depending on whether the reaction generates respectively a maximum or a minimum in the spatial viscosity profile.

Experiments are carried out in a horizontal Hele-Shaw (HS) cell consisting of two transparent glass plates 100 mm wide, 500 mm long, and 14 mm thick separated by a gap width $b = 0.25$ mm. This gap width is fixed by U shaped Teflon spacers closing one of the two small sides and both long sides of the cell. The open small side of length $l = 80$ mm is connected to a two-way valve providing a linear injection of fluid with a constant flow rate q [23]. Fluids are evacuated at the other lateral side through a 2-mm-radius hole in the bottom plate located at half the width and 20 mm before the closed side. The experiment is mounted on a lighting table providing uniform diffuse white light from below. Dynamics are recorded by a charge-coupled device camera fixed above the HS cell.

First, we demonstrate chemically induced VF in the case where the reaction produces a more viscous product. To do so, we use as the displacing more viscous fluid A a 0.30 wt% aqueous solution of polyacrylic acid (PAA) of molecular weight 1 250 000 (Sigma-Aldrich). The displaced less viscous fluid is either pure water or an aqueous solution of reactant B, chosen here as sodium hydroxide NaOH dyed by 0.04 wt% Trypan Blue, TB (Aldrich).

When the displaced fluid is dyed water, the interface remains stable and hence planar [see Fig. 1(a)] as expected for a solution of a polymer displacing less viscous water. This shows also that, although the polymer solution has shear thinning viscosity effects [24], such effects are not the origin of an instability here. If, now, the displaced fluid is a dyed aqueous solution of NaOH [Figs. 1(b) and 1(c)], the front becomes unstable with fingers developing behind the reactive interface. For increasing concentrations of NaOH, fingers extend here further backward and the instability develops earlier. Note that the instability cannot result from pure reaction-diffusion processes as $A + B \to C$ fronts are known to be unable to feature transverse instabilities [25]. Besides, in horizontal Hele-Shaw cells, such fronts are observed to travel without any transverse deformation if no injection takes place [26]. Moreover, in the absence of instability, the interface
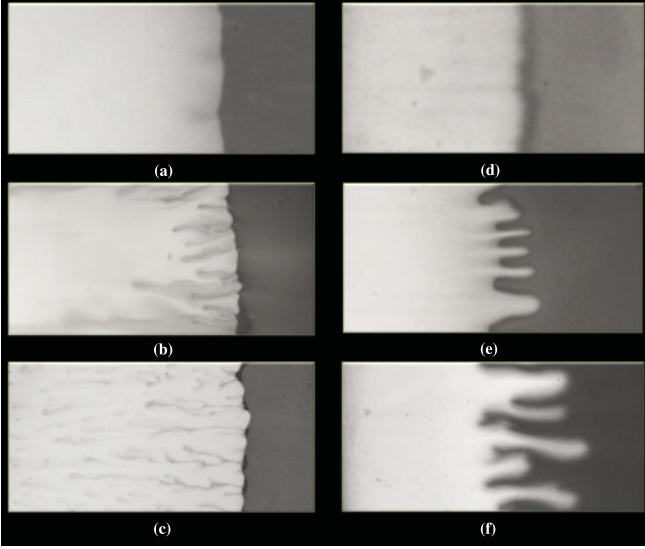
FIG. 1. Reaction driven VF when a polymer solution displaces linearly from left to right a less viscous aqueous dyed solution. Left: PAA displacing NaOH in concentration (a) 0 M, no fingering is observed; (b) 0.01 M; (c) 0.06 M. Flow rate $q = 0.5$ ml/min, time $t = 225$ s. Right: SPA displacing aqueous solutions of 60 wt% glycerol + HCl in concentration (a) 0 M; (b) 0.3 M; (c) 0.5 M. Flow rate $q = 0.25$ ml/min, time $t = 360$ s. Field of view = 4 cm $\times$ 8cm.

broadens on a diffusive time scale (of the order of hours), which is much slower than the chemical time scale (of the order of milliseconds). Indeed, we have here an acid-base reaction which proceeds quasi-instantaneously. The fact that the instability is observed on a time scale of a few seconds points to the fact that the mechanism of the instability is driven by convection and not by diffusion.

The presence of NaOH induces VF because the neutralization reaction PAA + NaOH $\rightarrow$ SPA + H$_2$O transforms the acid PAA into the more viscous salt sodium polyacrylate (SPA) and hence modifies the viscosity profile in the system. To quantify this aspect, we reconstruct quantitatively viscosity profiles by considering the dimensionless reaction-diffusion-convection model governing the evolution of the flow velocity **u** and of the dimensionless concentrations A, B, C of the chemical species [21,22]:

$$\nabla \cdot \mathbf{u} = 0; \quad \nabla p = -\mu \mathbf{u}; \tag{1}$$

$$\frac{\partial A}{\partial t} + \mathbf{u} \cdot \nabla A = \delta_A \nabla^2 A - D_a A B, \tag{2}$$

$$\frac{\partial B}{\partial t} + \mathbf{u} \cdot \nabla B = \delta_B \nabla^2 B - D_a A B, \tag{3}$$

$$\frac{\partial C}{\partial t} + \mathbf{u} \cdot \nabla C = \nabla^2 C + D_a A B, \tag{4}$$

$$\frac{\partial E}{\partial t} + \mathbf{u} \cdot \nabla E = \delta_E \nabla^2 E, \tag{5}$$

$$\mu = \exp(R_a A + R_c C), \tag{6}$$

where p is the pressure, D_a is the Damköhler number, $\delta_{A,B,E} = D_{A,B,E}/D_C$ are the ratio of diffusion coefficients, μ the viscosity and $R_{a,c}$ the log-mobility ratios [21,22]. Here E is a passive dye or glycerol added into the displaced solution
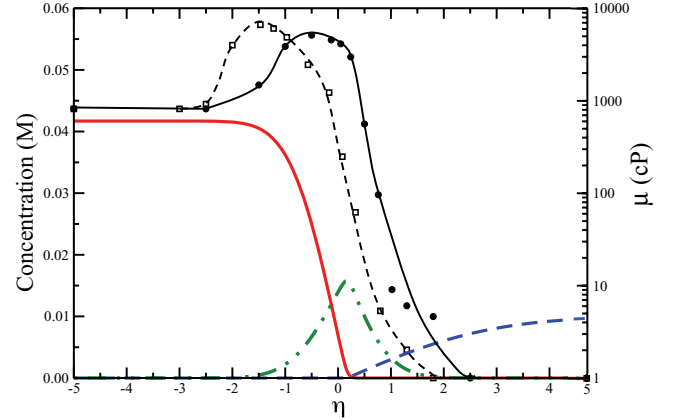

FIG. 2. (Color online) Quantitative concentration profiles reconstructed from the RD model (2)–(4) when a 0.30 wt% (0.042 M) solution of PAA displaces water + NaOH 0.01 M (full red line: PAA; blue dashed line: NaOH; green dashed-dotted line: SPA) and viscosity profiles for NaOH 0.01 M (line with filled circles) and NaOH 0.06 M (dashed line with open squares).

to visualize the pattern or change the viscosity as in the experiments. Equations have been scaled by the diffusion coefficient of the product C and the viscosity of the displaced solution of B as its viscosity remains constant and equal to that of water in the course of the experiments. We fix here $D_a = 1, \delta_A = 1, \delta_B = 10, \delta_E = 10$. The ratio of initial concentrations $\varphi = B_0/A_0$.

In the absence of flow (**u** = 0), these equations can be solved numerically to reconstruct dimensional asymptotic concentration profiles as a function of the self-similar variable $\eta = x/(4D_B t)^{1/2}$ (Fig. 2). Specific points are then chosen along these profiles and solutions containing a mix of PAA, SPA, and NaOH in the relevant proportions are then prepared. The viscosity of these solutions is measured as a function of the shear rate using a rotational viscosimeter (Brookfield, Pro Extra II). As the fluids are displaced linearly at a constant injection speed U in the Hele-Shaw cell, the corresponding shear rate $\dot{\gamma}$ is constant and shear thinning effects are certainly excluded. The shear rate can be estimated as $\dot{\gamma} = 2U/b = 2q/lb^2$ [9,13,14] where $l = 80$ mm is the width of the cell. Here $q = 0.50$ ml/min such that $\dot{\gamma} \sim 3.33$ s^{-1}. The corresponding viscosity of the pure 0.30 wt% PAA reactant solution is roughly 870 centipoise (cp) while that of the displaced fluid, with or without NaOH, is approximately equal to 1 cp (see Fig. 2). The viscosity in the reactive zone at the above chosen experimental points shown in Fig. 2 can rise up to 3880 cp, i.e., it is indeed much larger than that of both reactants.

Figure 2 shows thus quantitatively that, as soon as the reactive solutions are in contact, a viscosity maximum develops in the reaction zone, where PAA reacts with NaOH to produce more viscous SPA. The larger the concentration of sodium hydroxide in the displaced fluid, the larger the intensity of this maximum. Therefore, for a fixed time, we observe that increasing the reactant concentration from 0.01 to 0.06 M in the displaced fluid makes the interface more unstable [Figs. 1(b) and 1(c)], which is consistent with theoretical predictions [22]. Figure 2 shows that the locally unstable region of the nonmonotonic viscosity profile [27,28] is located behind

the reaction zone. This explains why fingers extend behind the interface as seen in the experiments [Figs. 1(b) and 1(c)]. To confirm this, we have integrated model (1)–(6) numerically for values of parameters of the experiments using the numerical scheme explained in Ref. [22]. Figure 4(a) shows that indeed fingers extending behind the reaction zone are observed.

Theoretical predictions suggest that reactions generating a product less viscous than the displaced fluid are also prone to destabilize an otherwise hydrodynamically stable configuration. To experimentally demonstrate this situation, we performed the same type of experiments as above, choosing now as the displacing fluid a 0.125 wt% aqueous solution of SPA (with molecular weight 2 100 000–6 600 000 from Wako) and, as the displaced reactant, an aqueous mixture of HCl and 60 wt% glycerol dyed by 0.04 wt% TB. The reaction is SPA $+ \, HCl \rightarrow PAA + NaCl$. The glycerol, which is passive to the reaction, is added in order to raise the viscosity of the displaced solution. Indeed in the absence of such glycerol, it would be very challenging to find reactions able to lower the viscosity below that of water.

When the displaced fluid is only dyed water and glycerol, the interface remains stable and hence planar, as shown in Fig. 1(d). However, if HCl is added to the displaced solution, the front becomes unstable and fingering developing ahead of the interface is observed [Figs. 1(e) and 1(f)]. Measurements of the viscosity have been performed as explained above at specific proportions of concentrations of SPA, HCl, PAA, and glycerol dictated by the numerical reaction-diffusion profiles shown in Fig. 3. Here, $q = 0.25$ ml/min, such that $\dot{\gamma} \sim 1.67$ s^{-1}. The corresponding viscosity of the pure 0.125 wt% SPA solution is 794 cp, the one of the displaced solution (aqueous solution of TB + glycerol with or without HCl) is approximately 10 cp while it falls to roughly 6 or 5 cp in the reaction zone in the presence of 0.3 or 0.5 M HCl respectively.

Thus the nonreactive condition is stable as we have a polymer SPA solution displacing a less viscous solution, however due to the chemical reaction at the interface, the neutralization of SPA by HCl leads to a local minimum

FIG. 4. (Color online) Numerical pattern of the dye concentration E on a dimensionless domain of width 2048 at $t = 2400$ for reaction-driven VF with (a) a maximum in viscosity, $R_a = 1, R_c = 6$, $\varphi = 1.44$; (b) a minimum, $R_a = 1, R_c = -2, \varphi = 37.6$.

within the spatial viscosity profile. The concentration of HCl controls the value of the minimum reached within the interface (Fig. 3), which influences the patterns obtained as seen in
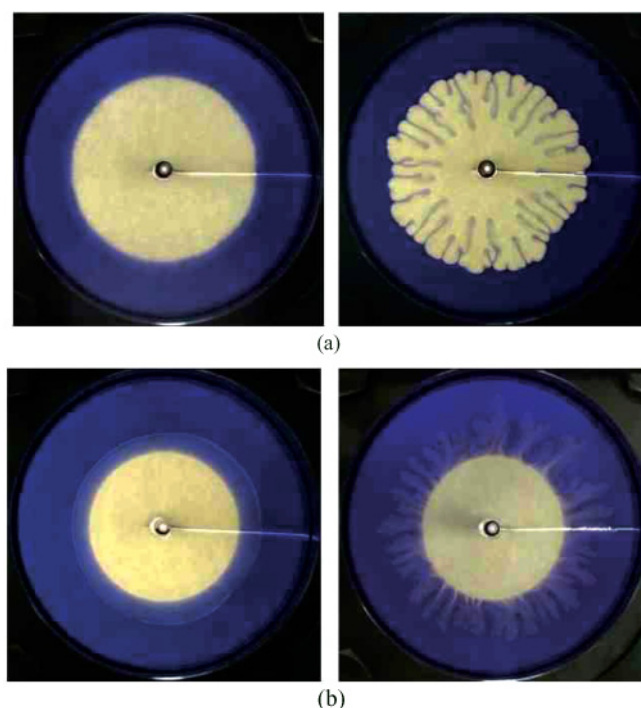
FIG. 5. (Color online) Radial displacement in a HS cell (gap = 0.5 mm). (a) PAA [Mw: 1 000 000 (Wako)] 1.0 wt% aqueous solution displacing a dyed aqueous solution without (left) or with NaOH 0.02 M (right), flow rate $q = 0.18$ ml/min. Time $t = 900$ s. (b) SPA [Mw: 2 100 000–6 600 000 (Wako)] 0.5 wt% aqueous solution SPA displacing a dyed aqueous solution 85% glycerol without (left) or with HCl 0.05 M (right), flow rate $q = 1.8$ ml/min. Time $t = 60$ s. Field of view = 11.6 cm × 11.6 cm.
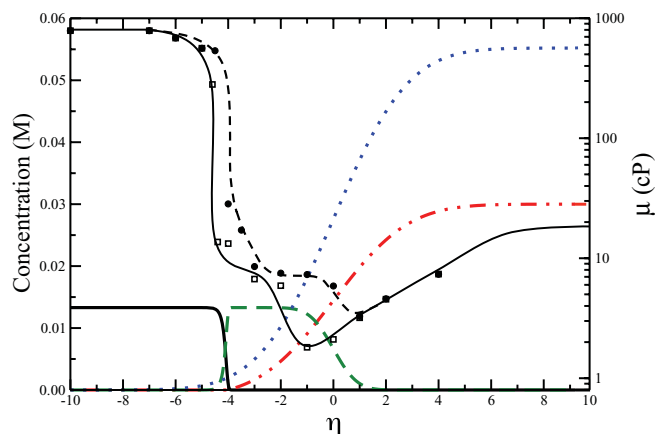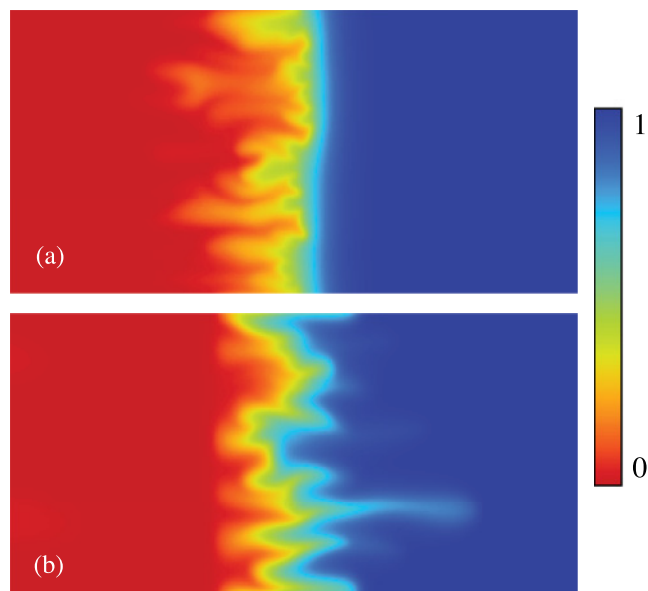

FIG. 3. (Color online) Quantitative concentration profiles when a 0.125 wt% solution of SPA displaces water + 60 wt% glycerol + HCl 0.3 M (full black line: SPA; red dashed-dotted line: HCl/10; blue dotted line: glycerol/100; green dashed line: PAA) and viscosity profiles for HCl 0.3 M (line with filled circles) and 0.5 M (line with open squares).

Figs. 1(e) and 1(f). The larger the amplitude of the minimum, the more unstable the system, which is consistent with the experimental observations. Note that the locally unfavorable viscosity contrast is here located ahead of the reaction zone, which explains why fingering is now observed ahead of the interface in both experiments [Figs. 1(e) and 1(f)] and numerical simulations [Fig. 4(b)].

A comparison of the viscosities reached in the reaction zone in both experiments shows that the unfavorable viscosity jump is much larger in the reaction of PAA with NaOH (Fig. 2) than for the reaction of SPA with HCl in the presence of glycerol (Fig. 3). Yet, the patterns appear on similar time scales. The difference can be attributed to the fact that fingering has been shown to be more intense in nonmonotonic profiles with a minimum when fingers extend along the flow rather than in the presence of a maximum when fingers develop against the flow and encounter a stable barrier in the streamwise direction [29].

Additionally, similar experiments made with a radial injection (Fig. 5) confirm that fingers extend preferably behind or ahead of the reaction zone depending whether the viscosity profile has a maximum or a minimum, respectively.

To summarize, we have provided experimental evidence of viscous fingering triggered by a reaction at the interface between a more viscous solution displacing a less viscous one in a Hele-Shaw cell. Such a situation is classically stable in the absence of a reaction. The chemical reaction, by generating a product either more or less viscous than both reactants, triggers in time a nonmonotonic viscosity profile. A locally unstable configuration with adverse mobility gradient develops around the extremum. This leads to fingers developing respectively behind or ahead of the reaction zone depending whether the viscosity profile exhibits a maximum or a minimum. These results pave the way to more detailed experimental analysis of scenarios in which chemical reactions (or other physical processes building up nonmonotonic viscosity profiles in time [30]) can destabilize otherwise classically viscous stable hydrodynamic situations.

[1] G. M. Homsy, Annu. Rev. Fluid Mech. **19**, 271 (1987).

[2] P. G. Saffman and G. I. Taylor, Proc. R. Soc. London, Ser. A **245**, 312 (1958).

[3] J. Nittmann, G. Daccord, and H. E. Stanley, Nature (London) **314**, 141 (1985).

[4] D. Bensimon, L. P. Kadanoff, S. Liang, B. I. Shraiman, and C. Tang, Rev. Mod. Phys. **58**, 977 (1986).

[5] Z. M. Yang, Y. C. Yortsos, and D. Salin, Adv. Water Resour. **25**, 885 (2002).

[6] A. De Wit, Y. Bertho, and M. Martin, Phys. Fluids **17**, 054114 (2005).

[7] A. Buka, J. Kertesz, and T. Vicsek, Nature (London) **323**, 424 (1986).

[8] K. Makino, M. Kawaguchi, K. Aoyama, and T. Kato, Phys. Fluids **7**, 455 (1995).

[9] D. H. Vlad and J. V. Maher, Phys. Rev. E **61**, 5439 (2000).

[10] D. Bonn, H. Kellay, M. Ben Amar, and J. Meunier, Phys. Rev. Lett. **75**, 2132 (1995).

[11] L. Kondic, M. J. Shelley, and P. Palffy-Muhoray, Phys. Rev. Lett. **80**, 1433 (1998).

[12] T. Podgorski, M. C. Sostarecz, S. Zorman, and A. Belmonte, Phys. Rev. E **76**, 016202 (2007).

[13] Y. Nagatsu, K. Matsuda, Y. Kato, and Y. Tada, J. Fluid Mech. **571**, 475 (2007).

[14] Y. Nagatsu, Y. Kondo, Y. Kato, and Y. Tada, J. Fluid Mech. **625**, 97 (2009).

[15] Y. Nagatsu, C. Iguchi, K. Matsuda, Y. Kato, and Y. Tada, Phys. Fluids **22**, 024101 (2010).

[16] A. De Wit and G. M. Homsy, J. Chem. Phys. **110**, 8663 (1999); Phys. Fluids **11**, 949 (1999).

[17] M. Mishra, M. Martin, and A. De Wit, Phys. Fluids **19**, 073101 (2007).

[18] T. Gérard and A. De Wit, Phys. Rev. E **79**, 016308 (2009).

[19] K. Ghesmat and J. Azaiez, Trans. Porous Media **77**, 489 (2009).

[20] S. H. Hejazi and J. Azaiez, Chem. Eng. Sci. **65**, 938 (2010).

[21] S. H. Hejazi, P. M. J. Trevelyan, J. Azaiez, and A. De Wit, J. Fluid Mech. **652**, 501 (2010).

[22] Y. Nagatsu and A. De Wit, Phys. Fluids **23**, 043103 (2011).

[23] R. Maes, G. Rousseaux, B. Scheid, M. Mishra, P. Colinet, and A. De Wit, Phys. Fluids **22**, 123104 (2010).

[24] S. Obernauer, G. Drazer, and M. Rosen, Physica A **283**, 187 (2000).

[25] L. Gálfi and Z. Rácz, Phys. Rev A **38**, 3151 (1988).

[26] Y. Shi and K. Eckert, Chem. Eng. Sci. **61**, 5523 (2006).

[27] O. Manickam and G. M. Homsy, Phys. Fluids **5**, 1356 (1993); **6**, 95 (1994).

[28] D. Schafroth, N. Goyal, and E. Meiburg, Eur. J. Mech. B **26**, 444 (2007).

[29] M. Mishra, M. Martin, and A. De Wit, Phys. Rev. E **78**, 066306 (2008).

[30] H. Tang, W. Grivas, D. Homentcovschi, J. Geer, and T. Singler, Phys. Rev. Lett. **85**, 2112 (2000).